

## Electronic band structure of Cu<sub>2</sub>O by spin density functional theory

This article has been downloaded from IOPscience. Please scroll down to see the full text article.

2009 J. Phys.: Condens. Matter 21 015502

(<http://iopscience.iop.org/0953-8984/21/1/015502>)

View [the table of contents for this issue](#), or go to the [journal homepage](#) for more

Download details:

IP Address: 129.252.86.83

The article was downloaded on 29/05/2010 at 16:54

Please note that [terms and conditions apply](#).

# Electronic band structure of Cu<sub>2</sub>O by spin density functional theory

M French, R Schwartz, H Stolz and R Redmer

Institut für Physik, Universität Rostock, D-18051 Rostock, Germany

E-mail: [ronald.redmer@uni-rostock.de](mailto:ronald.redmer@uni-rostock.de)

Received 7 October 2008

Published 1 December 2008

Online at [stacks.iop.org/JPhysCM/21/015502](http://stacks.iop.org/JPhysCM/21/015502)

## Abstract

The band structure of Cu<sub>2</sub>O is calculated using density functional theory in the generalized gradient approximation. By taking spin-orbit coupling into account the split between the  $\Gamma_7^+$  and the  $\Gamma_8^+$  valence band states is obtained as 128 meV. The highest valence band shows a noticeable nonparabolicity close to the  $\Gamma$  point. This is important for the quantitative description of excitons in this material, which is considered to be the best candidate for the confirmation that Bose-Einstein condensation also occurs in excitonic systems.

## 1. Introduction

Cuprous oxide, one of the first semiconductor materials, has enjoyed renewed interest in the last few years due to its promise as a material hosting Bose-Einstein condensation of excitons [1–3]. This is due to the unique properties of excitons in this material consisting of doubly degenerate electrons and holes at the  $\Gamma$  point. Coulomb attraction results in the formation of excitons showing a complete hydrogen-like Rydberg series with an unusual high 1s binding energy of 150 meV [4]. Recently, these transitions have been investigated by terahertz spectroscopy [5–7] which demonstrated nicely the hydrogen-like nature of these quasiparticles. Nevertheless, there are two fundamental limitations to the atom-like picture of excitons. Their energy dispersion is not strictly parabolic but stems from a possibly complex band structure, as is the case for most semiconductors like, for example, silicon or gallium arsenide. Furthermore, they are embedded in the background of a crystal lattice. Both effects are of especial importance for excitons with small Bohr radius comparable to the lattice constant, as is the case for Cu<sub>2</sub>O, since then Bloch functions from all over the first Brillouin zone contribute to the exciton wavefunction. Therefore, a quantitative study of exciton properties requires an accurate band structure including spin-orbit interaction.

Most of earlier band structure calculations for Cu<sub>2</sub>O [8–13] have neglected spin-orbit coupling. Only Kleinman and Mednick [14] have considered spin-orbit splitting at the  $\Gamma$  point perturbatively but not for the full band dispersion. It is the aim of the present study to perform an *ab initio* band structure calculation for Cu<sub>2</sub>O by taking into account spin-orbit coupling. The results of this calculation are expected

to put recent experimental and theoretical studies of the interexcitonic transitions in the terahertz regime [7, 15] on a more quantitative basis. This will allow more quantitative estimates of the possibility of a Bose-Einstein condensate in this material.

## 2. Details on the computational method

For our electronic band structure calculations we use density functional theory (DFT) including spin-orbit coupling, implemented in the Vienna *ab initio* simulation package (VASP) [16–19]. The generalized gradient approximation (GGA) of Perdew *et al* [20] is chosen for the exchange-correlation functional. We employ the standard PAW pseudopotentials [21, 22] provided with VASP. For each copper atom 10 electrons are considered in the DFT algorithm while 6 electrons are considered for each oxygen. Convergence tests have shown that a plane-wave cutoff of 600 eV and a Monkhorst-Pack [23]  $k$ -point grid of  $6 \times 6 \times 6$  are sufficient for a well-converged ground state energy of a single unit cell. The value of  $a = 4.2696 \text{ \AA}$  [24] was chosen for the lattice constant. Spin-exchange splitting is not observed. The bands are pairwise-degenerate except for energy differences of 0.3 meV or less, which is due to the limits of numerical accuracy. An introduction to the details of spin-DFT can be found, for example, in [25] and [26].

## 3. Band structure of Cu<sub>2</sub>O

The resulting band structure is plotted in figure 1. Visually comparing our band structure to previous results, the band structure of Ching *et al* [10] is the most similar one.

**Table A.1.** Eigenvalues  $E(k_x)$  of three valence and conduction bands along the  $\Delta$  line (from the  $\Gamma$  point to the X point,  $k_y = 0, k_z = 0$ ).

| $k_x$ ( $\pi/a$ ) | $E_{v3}$ (eV) | $E_{v2}$ (eV) | $E_{v1}$ (eV) | $E_{c1}$ (eV) | $E_{c2}$ (eV) | $E_{c3}$ (eV) |
|-------------------|---------------|---------------|---------------|---------------|---------------|---------------|
| 0/20              | 2.3597        | 2.3597        | 2.4878        | 2.9395        | 3.6714        | 3.6719        |
| 1/20              | 2.3348        | 2.3582        | 2.4763        | 2.9449        | 3.6823        | 3.7087        |
| 2/20              | 2.2556        | 2.3538        | 2.4573        | 2.9613        | 3.7131        | 3.8083        |
| 3/20              | 2.1319        | 2.3464        | 2.4418        | 2.9886        | 3.7638        | 3.9486        |
| 4/20              | 1.9837        | 2.3361        | 2.4275        | 3.0266        | 3.8332        | 4.1109        |
| 5/20              | 1.8247        | 2.3230        | 2.4120        | 3.0751        | 3.9202        | 4.2821        |
| 6/20              | 1.6625        | 2.3072        | 2.3945        | 3.1339        | 4.0234        | 4.4530        |
| 7/20              | 1.5021        | 2.2888        | 2.3746        | 3.2027        | 4.1415        | 4.6165        |
| 8/20              | 1.3469        | 2.2680        | 2.3522        | 3.2808        | 4.2733        | 4.7663        |
| 9/20              | 1.2003        | 2.2450        | 2.3275        | 3.3679        | 4.4177        | 4.8969        |
| 10/20             | 1.0672        | 2.2201        | 2.3005        | 3.4633        | 4.5737        | 5.0034        |
| 11/20             | 0.9623        | 2.1936        | 2.2715        | 3.5661        | 4.7405        | 5.0822        |
| 12/20             | 0.9431        | 2.1662        | 2.2409        | 3.6756        | 4.9173        | 5.1311        |
| 13/20             | 0.9905        | 2.1384        | 2.2091        | 3.7908        | 5.1037        | 5.1500        |
| 14/20             | 1.0368        | 2.1112        | 2.1767        | 3.9106        | 5.1400        | 5.2990        |
| 15/20             | 1.0802        | 2.0855        | 2.1446        | 4.0340        | 5.1039        | 5.5028        |
| 16/20             | 1.1185        | 2.0629        | 2.1137        | 4.1598        | 5.0452        | 5.7148        |
| 17/20             | 1.1497        | 2.0447        | 2.0855        | 4.2865        | 4.9676        | 5.9346        |
| 18/20             | 1.1718        | 2.0326        | 2.0613        | 4.4127        | 4.8748        | 6.1620        |
| 19/20             | 1.1832        | 2.0280        | 2.0428        | 4.5367        | 4.7702        | 6.3968        |
| 20/20             | 1.1832        | 2.0313        | 2.0315        | 4.6565        | 4.6567        | 6.6382        |

**Table A.2.** Eigenvalues  $E(k_x)$  of three valence and conduction bands along the  $\Sigma$  line (from the  $\Gamma$  point to the M point,  $k_y = k_x, k_z = 0$ ).

| $k_x$ ( $\pi/a$ ) | $E_{v3}$ (eV) | $E_{v2}$ (eV) | $E_{v1}$ (eV) | $E_{c1}$ (eV) | $E_{c2}$ (eV) | $E_{c3}$ (eV) |
|-------------------|---------------|---------------|---------------|---------------|---------------|---------------|
| 0/30              | 2.3597        | 2.3597        | 2.4878        | 2.9395        | 3.6714        | 3.6719        |
| 1/30              | 2.3417        | 2.3551        | 2.4765        | 2.9443        | 3.6871        | 3.6989        |
| 2/30              | 2.2875        | 2.3402        | 2.4511        | 2.9589        | 3.7311        | 3.7742        |
| 3/30              | 2.2023        | 2.3129        | 2.4251        | 2.9832        | 3.8000        | 3.8850        |
| 4/30              | 2.0972        | 2.2737        | 2.4034        | 3.0169        | 3.8885        | 4.0187        |
| 5/30              | 1.9828        | 2.2270        | 2.3845        | 3.0601        | 3.9917        | 4.1663        |
| 6/30              | 1.8663        | 2.1772        | 2.3661        | 3.1122        | 4.1052        | 4.3211        |
| 7/30              | 1.7526        | 2.1273        | 2.3470        | 3.1730        | 4.2249        | 4.4789        |
| 8/30              | 1.6449        | 2.0792        | 2.3265        | 3.2419        | 4.3471        | 4.6364        |
| 9/30              | 1.5457        | 2.0340        | 2.3043        | 3.3180        | 4.4684        | 4.7910        |
| 10/30             | 1.4562        | 1.9922        | 2.2803        | 3.4006        | 4.5849        | 4.9409        |
| 11/30             | 1.3771        | 1.9540        | 2.2547        | 3.4885        | 4.6928        | 5.0845        |
| 12/30             | 1.3084        | 1.9195        | 2.2276        | 3.5804        | 4.7879        | 5.2206        |
| 13/30             | 1.2491        | 1.8887        | 2.1990        | 3.6751        | 4.8663        | 5.3482        |
| 14/30             | 1.1984        | 1.8614        | 2.1691        | 3.7707        | 4.9243        | 5.4668        |
| 15/30             | 1.1550        | 1.8375        | 2.1382        | 3.8657        | 4.9594        | 5.5759        |
| 16/30             | 1.1179        | 1.8170        | 2.1065        | 3.9580        | 4.9706        | 5.6755        |
| 17/30             | 1.0865        | 1.7998        | 2.0743        | 4.0455        | 4.9588        | 5.7656        |
| 18/30             | 1.0630        | 1.7857        | 2.0417        | 4.1261        | 4.9265        | 5.8464        |
| 19/30             | 1.0670        | 1.7747        | 2.0092        | 4.1975        | 4.8777        | 5.9183        |
| 20/30             | 1.0894        | 1.7667        | 1.9770        | 4.2576        | 4.8166        | 5.9817        |
| 21/30             | 1.1107        | 1.7614        | 1.9454        | 4.3047        | 4.7480        | 6.0371        |
| 22/30             | 1.1287        | 1.7586        | 1.9148        | 4.3378        | 4.6759        | 6.0850        |
| 23/30             | 1.1432        | 1.7577        | 1.8856        | 4.3571        | 4.6043        | 6.1259        |
| 24/30             | 1.1543        | 1.7584        | 1.8583        | 4.3640        | 4.5363        | 6.1603        |
| 25/30             | 1.1626        | 1.7601        | 1.8335        | 4.3612        | 4.4746        | 6.1886        |
| 26/30             | 1.1683        | 1.7623        | 1.8118        | 4.3520        | 4.4213        | 6.2113        |
| 27/30             | 1.1718        | 1.7646        | 1.7938        | 4.3402        | 4.3782        | 6.2285        |
| 28/30             | 1.1735        | 1.7665        | 1.7804        | 4.3291        | 4.3465        | 6.2406        |
| 29/30             | 1.1733        | 1.7679        | 1.7720        | 4.3214        | 4.3270        | 6.2479        |
| 30/30             | 1.1714        | 1.7686        | 1.7688        | 4.3193        | 4.3199        | 6.2506        |

The experimental bandgap at the  $\Gamma$  point is known to be 2.1720 eV [27]. Our spin-DFT calculations indicate a bandgap of 0.45 eV while a value of 0.53 eV has been found for the spin-degenerate calculations. A recent theoretical study on  $\text{Cu}_2\text{O}$  doped with transition metal atoms [28], employing VASP in the spin-degenerate GGA +  $U$  approximation, has obtained a similar value of 0.48 eV for the pure crystal. It is well known that theoretical values derived from the GGA are too

small. Self-consistent GW calculations [12] yield the right bandgap. For our purposes, however, it is not necessary to do such computationally costly calculations, since the GW approximation mainly shifts the energies of the bands while its influence on the band dispersion is much smaller.

A closer extract around the Fermi energy, displaying the comparison between the spin-DFT calculations with the spin-degenerate case, is shown in figure 2. However, the

**Table A.3.** Eigenvalues  $E(k_x)$  of three valence and conduction bands along the  $\Lambda$  line (from the  $\Gamma$  point to the  $R$  point,  $k_y = k_z = k_x$ ).

| $k_x$ ( $\pi/a$ ) | $E_{v3}$ (eV) | $E_{v2}$ (eV) | $E_{v1}$ (eV) | $E_{c1}$ (eV) | $E_{c2}$ (eV) | $E_{c3}$ (eV) |
|-------------------|---------------|---------------|---------------|---------------|---------------|---------------|
| 0/40              | 2.3597        | 2.3597        | 2.4878        | 2.9395        | 3.6714        | 3.6719        |
| 1/40              | 2.3460        | 2.3545        | 2.4779        | 2.9436        | 3.6895        | 3.6900        |
| 2/40              | 2.3073        | 2.3365        | 2.4534        | 2.9559        | 3.7401        | 3.7418        |
| 3/40              | 2.2493        | 2.3000        | 2.4261        | 2.9764        | 3.8178        | 3.8209        |
| 4/40              | 2.1786        | 2.2442        | 2.4039        | 3.0049        | 3.9159        | 3.9202        |
| 5/40              | 2.1011        | 2.1762        | 2.3855        | 3.0414        | 4.0283        | 4.0336        |
| 6/40              | 2.0213        | 2.1035        | 2.3682        | 3.0857        | 4.1504        | 4.1561        |
| 7/40              | 1.9426        | 2.0309        | 2.3502        | 3.1376        | 4.2783        | 4.2842        |
| 8/40              | 1.8672        | 1.9615        | 2.3308        | 3.1966        | 4.4092        | 4.4150        |
| 9/40              | 1.7971        | 1.8971        | 2.3096        | 3.2625        | 4.5408        | 4.5461        |
| 10/40             | 1.7333        | 1.8388        | 2.2865        | 3.3347        | 4.6709        | 4.6757        |
| 11/40             | 1.6765        | 1.7872        | 2.2613        | 3.4127        | 4.7979        | 4.8019        |
| 12/40             | 1.6271        | 1.7425        | 2.2342        | 3.4958        | 4.9203        | 4.9232        |
| 13/40             | 1.5853        | 1.7046        | 2.2050        | 3.5836        | 5.0364        | 5.0382        |
| 14/40             | 1.5508        | 1.6733        | 2.1739        | 3.6751        | 5.1451        | 5.1455        |
| 15/40             | 1.5236        | 1.6483        | 2.1408        | 3.7696        | 5.2438        | 5.2451        |
| 16/40             | 1.5032        | 1.6290        | 2.1060        | 3.8664        | 5.3320        | 5.3352        |
| 17/40             | 1.4893        | 1.6152        | 2.0696        | 3.9646        | 5.4090        | 5.4145        |
| 18/40             | 1.4815        | 1.6065        | 2.0316        | 4.0633        | 5.4737        | 5.4818        |
| 19/40             | 1.4793        | 1.6024        | 1.9924        | 4.1614        | 5.5252        | 5.5363        |
| 20/40             | 1.4821        | 1.6026        | 1.9523        | 4.2580        | 5.5625        | 5.5771        |
| 21/40             | 1.4894        | 1.6066        | 1.9115        | 4.3519        | 5.5852        | 5.6035        |
| 22/40             | 1.5004        | 1.6140        | 1.8705        | 4.4416        | 5.5927        | 5.6151        |
| 23/40             | 1.5145        | 1.6244        | 1.8296        | 4.5256        | 5.5852        | 5.6119        |
| 24/40             | 1.5312        | 1.6374        | 1.7895        | 4.6025        | 5.5635        | 5.5944        |
| 25/40             | 1.5498        | 1.6525        | 1.7507        | 4.6706        | 5.5289        | 5.5639        |
| 26/40             | 1.5699        | 1.6686        | 1.7143        | 4.7286        | 5.4835        | 5.5222        |
| 27/40             | 1.5910        | 1.6722        | 1.6939        | 4.7756        | 5.4296        | 5.4717        |
| 28/40             | 1.6126        | 1.6430        | 1.7100        | 4.8117        | 5.3700        | 5.4148        |
| 29/40             | 1.6138        | 1.6345        | 1.7300        | 4.8376        | 5.3069        | 5.3540        |
| 30/40             | 1.5878        | 1.6562        | 1.7507        | 4.8548        | 5.2429        | 5.2917        |
| 31/40             | 1.5663        | 1.6774        | 1.7717        | 4.8650        | 5.1800        | 5.2300        |
| 32/40             | 1.5543        | 1.6977        | 1.7926        | 4.8699        | 5.1201        | 5.1705        |
| 33/40             | 1.5761        | 1.7168        | 1.8131        | 4.8711        | 5.0649        | 5.1147        |
| 34/40             | 1.6248        | 1.7343        | 1.8332        | 4.8691        | 5.0163        | 5.0640        |
| 35/40             | 1.6732        | 1.7499        | 1.8525        | 4.8641        | 4.9762        | 5.0194        |
| 36/40             | 1.7148        | 1.7632        | 1.8707        | 4.8553        | 4.9465        | 4.9817        |
| 37/40             | 1.7474        | 1.7739        | 1.8872        | 4.8433        | 4.9279        | 4.9517        |
| 38/40             | 1.7704        | 1.7817        | 1.9007        | 4.8310        | 4.9179        | 4.9298        |
| 39/40             | 1.7838        | 1.7865        | 1.9097        | 4.8223        | 4.9133        | 4.9166        |
| 40/40             | 1.7881        | 1.7882        | 1.9129        | 4.8191        | 4.9119        | 4.9121        |

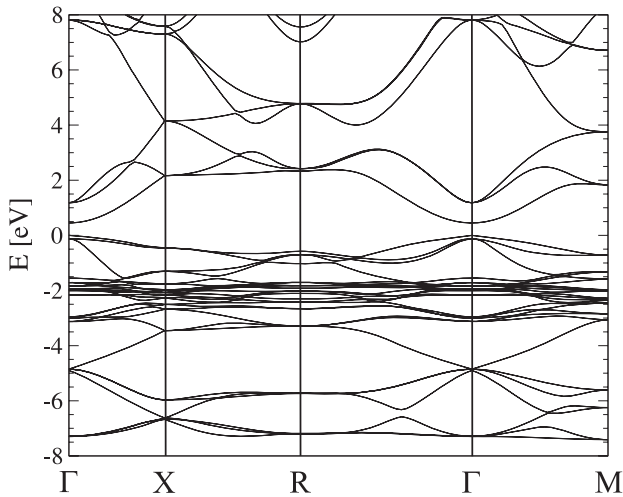


**Figure 1.** Electronic band structure of  $\text{Cu}_2\text{O}$ . The Fermi level is at zero energy.

otherwise sixfold-degenerate upmost valence band in the  $\Gamma$  point splits into two  $\Gamma_7^+$  states and four  $\Gamma_8^+$  states separated by a gap of 128 meV. This value is in very good agreement

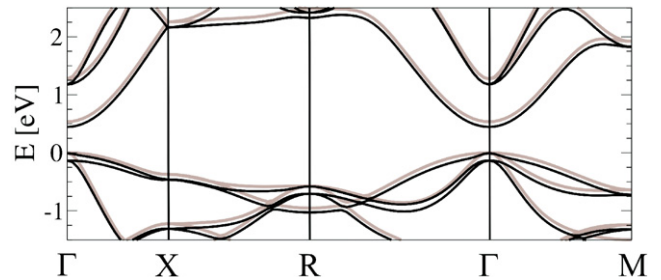


**Figure 2.** Comparison of the band structure including spin-orbit coupling (black) to calculations neglecting it (grey). Both sets of eigenvalues are normalized with the Fermi levels at zero energy.

with the value of 127.3 meV of Kleinman and Mednick [14] obtained in a perturbative approach as well as the estimate of Elliott [29] of 130 meV. The experimental value is 133.8 meV [27]. Furthermore, the highest valence band shows a strong nonparabolicity close to the  $\Gamma$  point which does not occur in the spin-degenerate calculations. We have listed the eigenvalues of the three valence and conduction bands near the Fermi energy in the appendix.

## 4. Conclusions

We have calculated the band structure of Cu<sub>2</sub>O within the spin-DFT in the generalized gradient approximation and taken spin-orbit coupling into account. Using these calculations it should be possible to derive improved values of effective masses and nonparabolicity parameters of the highest valence bands and thus allow more realistic descriptions of state-of-the-art models for excitonic transitions in the THz regime and also for a better understanding of BEC in excitonic systems.

## Acknowledgments

We thank B Holst for helpful comments. This work was supported by the DFG within the SFB 652 and the Supercomputing Center North (HLRN) in Germany.

## Appendix. Tabulated eigenvalues of bands

Tables A.1–A.3 contain the eigenvalues of three valence and conduction bands on high symmetry lines from the Brillouin zone centre.

## References

- [1] Snoke D 2002 *Science* **298** 1368
- [2] Lin J L and Wolfe J P 1993 *Phys. Rev. Lett.* **71** 1222
- [3] Zimmermann R 2007 *Problems of Condensed Matter Physics—Quantum Coherence Phenomena in Electron–Hole and Coupled Matter–Light Systems* ed A L Ivanov and S G Tikhodeev (Oxford: Oxford University Press) p 281
- [4] Grun J B, Sieskind M and Nikitine J 1961 *J. Phys. Chem. Solids* **19** 189
- [5] Kuwata-Gonokami M, Kubouchi M, Shimano R and Mysyrowicz A 2004 *J. Phys. Soc. Japan* **73** 1065
- [6] Jörgler M, Fleck T, Klingshirn C and von Baltz R 2005 *Phys. Rev. B* **71** 235210
- [7] Huber R, Schmid B A, Shen Y R, Chemla D S and Kaindl R A 2006 *Phys. Rev. Lett.* **96** 017402
- [8] Robertson J 1983 *Phys. Rev. B* **28** 3378
- [9] Marksteiner P, Blaha P and Schwarz K 1986 *Z. Phys. B* **64** 119
- [10] Ching Y W, Xu Y N and Wong K W 1989 *Phys. Rev. B* **40** 7684
- [11] Ruiz E *et al* 1997 *Phys. Rev. B* **56** 7189
- [12] Bruneval F *et al* 2006 *Phys. Rev. Lett.* **97** 267601
- [13] Gordienko A B, Zhuravlev Yu N and Fedorov D G 2007 *Phys. Solid State* **49** 223
- [14] Kleinman L and Mednick K 1980 *Phys. Rev. B* **21** 1549
- [15] Koch S W 2008 private communication
- [16] Kresse G and Hafner J 1993 *Phys. Rev. B* **47** 558
- [17] Kresse G and Hafner J 1994 *Phys. Rev. B* **49** 14251
- [18] Kresse G and Furthmüller J 1996 *Phys. Rev. B* **54** 11169
- [19] Kresse G and Furthmüller J 1996 *Comput. Mater. Sci.* **6** 15
- [20] Perdew J P, Burke K and Ernzerhof M 1996 *Phys. Rev. Lett.* **77** 3865
- [21] Blöchl P E 1994 *Phys. Rev. B* **50** 17953
- [22] Kresse G and Joubert D 1999 *Phys. Rev. B* **59** 1758
- [23] Monkhorst H J and Pack J D 1976 *Phys. Rev. B* **13** 5188
- [24] Swanson H E and Fuyat R K 1953 *NBS Circular* **539** II 23
- [25] Zeller R 2006 Spin-Polarized DFT Calculations and Magnetism *Computational Nanoscience: Do It Yourself (NIC Series 31)* ed J Grotendorst, S Blugel and D Marx (Jülich: John von Neumann Institute for Computing) pp 419–45
- [26] Bihlmayer G 2006 Non-Collinear Magnetism: Exchange Parameter and  $T_C$  *Computational Nanoscience: Do It Yourself (NIC Series 31)* ed J Grotendorst, S Blugel and D Marx (Jülich: John von Neumann Institute for Computing) pp 447–67
- [27] Uihlein Ch, Fröhlich D and Kenklies R 1981 *Phys. Rev. B* **23** 2731
- [28] Sieberer M, Redinger J and Mohn P 2007 *Phys. Rev. B* **75** 035203
- [29] Elliott R J 1961 *Phys. Rev.* **124** 340